Data paper

The International Journal of Robotics Research
2024, Vol. 43(5) 591–601

DOI: 10.1177/02783649231210011
journals.sagepub.com/home/ijr

MAgro dataset: A dataset for simultaneous localization and mapping in agricultural environments

Mercedes Marzoa Tanco[1], Guillermo Trinidad Barnech[1], Federico Andrade[1], Javier Baliosian[1,*], Martin LLofriu[1,*], JM Di Martino[2,*] and Gonzalo Tejera[1,*]

Abstract

The agricultural industry is being transformed, thanks to recent innovations in computer vision and deep learning. However, the lack of specific datasets collected in natural agricultural environments is, arguably, the main bottleneck for novel discoveries and benchmarking. The present work provides a novel dataset, Magro, and a framework to expand data collection. We present the first version of the Magro Dataset V1.0, consisting of nine ROS bags (and the corresponding raw data) containing data collected in apple and pear crops. Data were gathered, repeating a fixed trajectory on different days under different illumination and weather conditions. To support the evaluation of loop closure algorithms, the trajectories are designed to have loop closures, revisiting some places from different viewpoints. We use a Clearpath's Jackal robot equipped with stereo cameras pointing to the front and left side, a 3D LIDAR, three inertial measurement units (IMU), and wheel encoders. Additionally, we provide calibrated RTK GPS data that can be used as ground truth. Our dataset is openly available, and it will be updated to have more data and variability. Finally, we tested two existing state-of-the-art algorithms for vision and point cloud-based localization and mapping on our novel dataset to validate the dataset's usability.

Keywords

dataset, simultaneous localization and mapping, agricultural automation

Received 28 March 2023; Revised 20 September 2023; Accepted 27 September 2023
Senior Editor: Tim Barfoot
Associate Editor: Marjia Popovic

1. Introduction

In recent years, the use of technology in agriculture has grown significantly motivated by improving productivity and resource optimization (Roldán et al., 2018). Technology helps reduce the use of fertilizers, pesticides (Mogili and Deepak, 2018), and water wastage (Pawlowski et al., 2017). Agricultural activities significantly benefit from technology, including applying micronutrients (Lopez-Castro et al., 2020), estimating the quality and quantity of fruits (Gongal et al., 2018), and the mechanical or electromagnetic removal of weeds (Dhanasekar et al., 2022). Robots can be helpful as autonomous platforms capable of performing the mentioned tasks and, in addition, can be used to acquire a continuously large amount of crop data.

A central aspect of carrying out these tasks is equipping a robot with autonomous navigation capabilities in an agricultural environment, including locating it precisely and estimating the odometry. These environments present particularly challenging characteristics, such as repetitive patterns due to the vegetation's lack of singular and consistent visual attributes, which poses unique challenges for loop-closure detection algorithms. Moreover, these natural environments present unique computer vision challenges due to the subtle movements caused by wind and irregular terrains, extreme light variability, and seasonal crop changes due to crop management and weather variability.

In a new era of algorithms based on deep learning, large and open datasets are crucial for developing data-driven solutions and benchmarks. Though rich datasets are available for urban environments, for example, (Geiger et al., 2013; Maddern et al., 2017), to the best of our knowledge, the largest datasets currently available for rural locations are the Rosario Dataset (Pire et al., 2019) and the Sugar Beets Dataset (Chebrolu et al., 2017) and there is a need for more datasets collected in outdoor rural scenes.

[1]Universidad de la República, Montevideo, Uruguay
[2]Duke University, Durham, NC, USA

*Co-senior authors

Corresponding author:
Mercedes Marzoa Tanco, Facultad de Ingeniería, Universidad de la República, Av. Julio Herrera y Reissig 565, Montevideo 11600, Uruguay.
Email: mmarzoa@fing.edu.uy

We present a data collection framework and a novel and dynamic dataset collected in agricultural environments over an entire crop season using the robot depicted in Figure 1. The data collected includes images from two stereo cameras, one capturing towards the front and one towards the left, a 3D LIDAR, inertial measurement unit (IMU), wheel encoders, and GPS-RTK as ground truth. This work provides unique data to improve the development of visual odometry; moreover, side camera views can be leveraged for the evaluation of geometric and semantic mapping tasks. It is important to note that the data was collected in a field of wall-shaped apple trees, as far as possible from other tall surrounding trees that might cause GPS signal degradation. In addition, this field has good cellular network coverage, which provides an adequate data connection to the base. We drove the same route under different conditions on different days, capturing data with variations in illumination, weather, and crop management activity. In addition to the sensor data, we explain how to calibrate sensors' intrinsic and extrinsic parameters and the tools to process the data. Samples of the data collected are shown in Figure 2.

The main contributions of this work can be summarized as follows: (i) we present a novel dataset with rich and challenging features, to the best of our knowledge, the only one composed of data taken with a front camera in an agricultural environment with loop closures, (ii) we developed and open-sourced our data collection pipeline, which will be used to augment and expand the dataset periodically, and (iii) we validated the suitability of the proposed dataset by running two state-of-the-art SLAM algorithms on it. The dataset, its downloading guide, and the tools to process it are publicly available in the dataset repository.[1]

We organize the rest of the paper as follows: we present related work in Section 2, focusing on outdoor datasets. In Section 3, we present the robot platform and calibration method. In Section 4, we present the data acquisition process and the data structure. In Section 5, we evaluate the dataset on state-of-the-art algorithms to validate its quality, and in Section 6, we present a summary and future work.

Figure 1. Robotic platform used to acquire data, equipped with two ZED 2 stereo cameras (frontal and lateral), a 3D Velodyne laser, an IMU, and a Leica RTK-GPS.

2. Related work

There are several datasets available that are of great importance in building location and mapping solutions. We can classify them according to whether they are synthetic or "real" and the type of scene. Synthetic datasets are generated by simulating a 3D virtual environment (i.e., object geometry and texture, the properties of the materials, lighting conditions, and camera model and parameters). On the other hand, we refer to datasets as "real" if they consist of sequences of images/videos collected in real-world environments using physical hardware (cameras, LIDAR sensors, GPS, and so forth). Table 1 summarizes the related datasets that are presented below.

2.1. Synthetic datasets

Wang et al. (2020a) proposed a dataset that uses rendered photorealistic images to evaluate VSLAM in indoor environments. In contrast, Ros et al. (2016) developed a synthetic collection of diverse urban images while Curnis et al. (2022) focused on outdoor non-urban environments. Wang et al. (2020b) focused on simulating photorealistic images under various illumination and weather conditions and considered moving objects designed to cover a wide range of scenes. Choi et al. (2023) presents a synthetic dataset featuring different types of plants. It includes RGB images, fruit labels, the camera position from which the images were taken, and pointers to other images that can be accessed by performing an action. Hroob et al. (2021) create a simulated vineyard environment and test SLAM algorithms in those environments.

Figure 2. Examples of the data collected by the robot. From left to right: front left RGB image, lateral left RGB image, Velodyne scan.

Table 1. Summary of the surveyed datasets. There is a focus on those made for SLAM or other agricultural tasks. Highlighted in gray are the most relevant, publicly available datasets produced from non-synthetic agricultural environments for SLAM tasks.

Dataset	Real/ synthetic	Indoor/ outdoor	Environment	Main task	RGB	Depth	GPS	IMU	LiDAR	Ground truth	Publicly available
Wang et al., (2020a)	Synthetic	Indoor	Garages	SLAM	Yes	Yes	No	No	No	Pose	No
Synthia Ros et al. (2016)	Synthetic	Outdoor	Urban	Semantic segmentation for navigation	Yes	Yes	No	No	No	Semantic label	Yes
GTASynth Curnis et al. (2022)	Synthetic	Outdoor	Non-urban	SLAM, pointcloud registration	Yes	No	No	No	Yes	Pose	Yes
TartanAir Wang et al. (2020b)	Synthetic	Both	All	SLAM	Yes	Yes	No	No	Yes	Pose	Yes
Davis-Ag Choi et al. (2023)	Synthetic	Outdoor	Agricultural	Fruit detection	Yes	No	No	No	No	Semantic label	Yes
Hroob et al. (2021)	Synthetic	Outdoor	Vineyard	SLAM	Yes	Yes	No	Yes	Yes	Pose	Yes
Capsicum annuum Barth et al. (2018)	Synthetic	Outdoor	Pepper plants	Semantic segmentation	Yes	Yes	No	No	No	Semantic label	Yes
Di Cicco et al. (2017)	Synthetic	Outdoor	Agricultural	SLAM, weed classification	Yes	No	No	No	No	Semantic label	No
EuRoC Burri et al. (2016)	Real	Indoor	Industrial & room	SLAM	Yes	Yes	No	Yes	No	Pose	Yes
Cold Pronobis and Caputo (2009)	Real	Indoor	Laboratory	SLAM	Yes	No	No	No	No	Pose	Yes
TUM Sturm et al. (2012)	Real	Indoor	Industrial & office	SLAM	Yes	Yes	No	No	No	Pose	Yes
Oxford RobotCar Maddern et al. (2017)	Real	Outdoor	Urban	SLAM	Yes	No	Yes	No	Yes	Pose	Yes
KITTI Geiger et al. (2013)	Real	Outdoor	Urban	SLAM	Yes	Yes	Yes	Yes	Yes	Pose	Yes
Majdik et al. (2017)	Real	Outdoor	Urban	SLAM	Yes	No	Yes	Yes	No	Pose	Yes
ADVIO Cortés et al. (2018)	Real	Both	Urban	VIO	Yes	No	No	No	No	Pose	Yes
PATHoBot Smitt et al. (2021)	Real	Indoor	Glasshouse	Fruit detection, 3D recosntruction	Yes	Yes	No	No	No	—	No
Symphony Lake Griffith et al. (2017)	Real	Outdoor	Lake	SLAM	Yes	No	Yes	Yes	Yes	Pose	Yes
The Visual-Inertial Canoe Miller et al. (2018)	Real	Outdoor	River	SLAM	Yes	Yes	Yes	Yes	No	Pose	Yes
CropRow detection de Silva et al. (2021)	Real	Outdoor	Sugar beet field	Semantic segmentation	Yes	No	No	No	No	Crop row	Yes
Aghi et al. (2021)	Real	Outdoor	Vineyard	Semantic segmentation	Yes	Yes	No	No	No	Semantic label	Yes
AgriPest Wang et al. (2021)	Real	Outdoor	Crops	Pest detection	Yes	No	No	No	No	Semantic label	Yes
Altaheri et al. (2019)	Real	Outdoor	Datepalm	Fruit detection	Yes	No	No	No	No	Semantic label	Yes

(continued)

Table 1. (continued)

Dataset	Real/ synthetic	Indoor/ outdoor	Environment	Main task	RGB	Depth	GPS	IMU	LiDAR	Ground truth	Publicly available
MinneApple Häni et al. (2020)	Real	Outdoor	Apples	Fruit detection	Yes	No	No	No	No	Semantic label	Yes
Perez-Borrero et al. (2020)	Real	Outdoor	Strawberry	Fruit detection	Yes	No	No	No	No	Semantic label	No
GrowliFlower Kierdorf et al. (2023)	Real	Outdoor	Cauliflower	Growth estimation	Yes	No	Yes	No	No	Semantic label	Yes
Agri-Robotic Polvara et al. (2022)	Real	Outdoor	Vineyard	SLAM	Yes	Yes	Yes	Yes	Yes	Pose	No
Sugar Beets Chebrolu et al. (2017)	Real	Outdoor	Sugar beet field	SLAM, weed classification	Yes	Yes	Yes	No	Yes	Pose	Yes
Rosario Pire et al. (2019)	Real	Outdoor	Soybean field	SLAM	Yes	Yes	Yes	Yes	No	Pose	Yes
Ours	Real	Outdoor	Apple field	SLAM	Yes	Yes	Yes	Yes	Yes	Pose	Yes

Different synthetic datasets have been proposed for agricultural tasks, for example, semantic segmentation (Barth et al., 2018) and weeding (Di Cicco et al., 2017).

2.2. Real datasets

Within these datasets, we can classify scenes as indoor or outdoor, being the outdoor ones classifiable according to whether they are recording urban locations or other types of environments.

2.2.1. Indoors. These datasets are among the most popular and easy to collect and process. Compared to outdoor settings, indoor scenes tend to present a reduced range of illumination. The elements are frequently fabricated, limiting the number of textures, and they are not affected heavily by sunlight, weather, or seasonal changes. There are several indoor datasets leveraging different platforms and sensors. Burri et al. (2016) used an aerial vehicle to acquire data through a stereo camera and IMU, Sturm et al. (2012) considered an RGB-D system mounted on a rigid frame and Pronobis and Caputo (2009) implemented a camera system used in different robotic platforms.

2.2.2. Outdoors. As described above, the present work focuses on outdoor settings. These can be further classified into "urban" or "natural," depending on whether the data recorded corresponds to urban or natural environments. We are particularly interested in the latter case since this study focuses on agricultural settings. However, as we discuss next, urban scenes received significantly more attention in recent years, motivated by the active novel industry of self-driven vehicles.

2.2.2.1. Urban. Maddern et al. (2017) presented a dataset collected using six (RGB) cameras, a LIDAR, and a GPS. Geiger et al. (2013) leverage high-resolution color and grayscale stereo cameras, a Velodyne 3D laser scanner, and a high-precision GPS/IMU. These works collected data using ground vehicles; a different approach is to use drones or other flying robots. An example is the work of Majdik et al. (2017); they recorded data flying within urban streets at low altitudes using a micro aerial vehicle equipped with high-resolution cameras, GPS, and IMU. Cortés et al. (2018) collected data asking pedestrians to record video with smartphone devices as they walked over different trajectories.

2.2.2.2. Natural. Griffith et al. (2017) recorded data on a lake over 3 years using a surface vehicle equipped with 2D LIDAR, an (RGB) camera, GPS, and an IMU. A similar approach was followed by Miller et al. (2018), who recorded data on the Sangamon River in Illinois (US) using a canoe equipped with a stereo camera, an IMU, and a GPS. More closely related to the present paper, Chebrolu et al. (2017) introduced a dataset for plant classification and mapping; they used an agricultural field robot with a 4-channel multispectral camera, an RGB-D sensor, multiple LIDARs, and a GPS to record data over 3 months on a sugar beet farm. In the same line, Pire et al. (2019) presented an agricultural dataset collected by a weed removal robot on a soybean field, equipped with a stereo camera, an IMU, wheel odometry, and a GPS-RTK as ground truth. Polvara et al. (2022) presents a long-term pipeline of data collection in vineyards, although they do not mention their dataset's availability.

There are also works that, although not originally made for SLAM, are related to visual navigation, such as de Silva et al. (2021), which creates a dataset of marked rows in a sugar beet field, Aghi et al. (2021), which creates a semantically segmented dataset of vineyard rows, and Smitt et al. (2021) which present an automated platform for surveying sweet pepper and tomato crops using a pipe-rail trolley with an array of RGB-D cameras and a tracking camera inside a greenhouse.

On the other hand, there are several agricultural datasets unrelated to the task of odometry, mapping or navigation, such as pest detection (Wang et al., 2021), insect pest recognition (Wang et al., 2021), harvest estimation (Altaheri et al., 2019; Häni et al., 2020), or fruit and plant detection (Kierdorf et al., 2023; Perez-Borrero et al., 2020), among others. Lu and Young (2020) present a survey of public datasets for computer vision tasks in precision agriculture.

To the best of our knowledge, the closest existing works to ours are the Rosario dataset (Pire et al., 2019), and the Sugar Beets dataset (Chebrolu et al., 2017). Our approach is similar in that all are composed of agriculture-georeferenced images taken by robots. Despite similarities, our work is unique as it presents images taken while navigating rows of trees, while the others focus on small plants like sugar beets or soybean fields. Also, while the Sugar Beets Dataset is based on cameras pointing to the floor, as they focus primarily on weed detection, we set the cameras aiming forward and sideways since our focus is autonomous vision-based navigation, localization, and odometry estimation. Another significant difference is that our work has loop closures, a critical feature in testing SLAM algorithms. To the best of our knowledge, the proposed dataset is the first to include loop closures in natural agricultural settings; moreover, it is the first publicly available dataset recorded while navigating fruit crops. Finally, we establish a data collection pipeline and provide video sequences collected over the same trajectory over different seasons. The work in Polvara et al. (2022) also seems to be highly related to ours and will be a significant input once published and available.

3. The robotic platform

The platform used to acquire the data is a Jackal robot from Clearpath Robotics. It is a 508 × 430 × 250 mm mobile platform with a high torque 4 × 4 drivetrain and a maximum speed of 2.0 m/s. Sensors are mounted on a wooden frame, allowing us to control their height and placement, as shown in Figure 1. The GPS is mounted on top of the same frame to maximize signal quality. The robot has two stereo cameras, one mounted looking forward and one looking to the left. There is also a LIDAR located in the middle of the wooden frame, below the front camera. The specifications of the sensors are included below.

- Stereo cameras: both stereo cameras are ZED2 from Stereolabs with embedded IMUs. We recorded left and right images of each stereo camera in a synchronized manner. These JPEG compressed (quality 80%) images with a resolution of 1280 × 720 × 3. The field of view is Max. 110° (H) × 70° (V) × 120° (D), and the depth range is 0.3 m to 20 m. We also recorded ZED2's IMU data at 315 Hz. The front camera was recorded at 18 fps, while the left one was at 6 fps.
- LIDAR: We use Velodyne's Puck 3D LIDAR with a range of 100 m and 360° horizontal field of view and a 30° vertical field of view (our particular setup has an occlusion caused by the supporting frame and by the movement of people behind the robot). It was recorded at 10 Hz.
- Inertial Measurement Unit: We used the IMU mounted on the Jackal platform at 68 Hz.
- Motor encoders: We used quadrature encoders mounted on Jackal at 78,000 pulses/m.
- GPS-RTK: To track the robot's position, we use a Leica GS08 CS15 Viva GPS-RTK, mounted on the robot, as ground truth, recorded at 1 Hz. The GPS only stores points with an error of less than 0.01 m.

Note that the cameras have a drop in fps due to the process of compression and recording to disk. Also, we prioritize the frontal camera, more critical for SLAM, over the side one, which is typically intended for the visual analysis of the plant and fruits. It should be noted that the synchronization of the sensors and the GPS is made using their timestamp.

3.1. Computing platform

We equipped our robot with a Jetson Xavier NX Developer Kit from NVIDIA that has 8 GB of RAM memory. It has a GPU with NVIDIA Volta architecture, 384 NVIDIA CUDA cores, 48 Tensor cores, and a 6-core NVIDIA Carmel ARM v8.2 64-bit CPU. It runs Ubuntu 18 and ROS Melodic.

3.2. Calibration

We calibrated intrinsic and extrinsic parameters, which are essential to combine sensor information. Intrinsic parameters do not depend on the environment and the position of the sensor; an example of this could be a camera's focal length or field of view. On the other hand, extrinsic parameters depend on the relative position of each sensor and the global reference frame defined. In this case, we calibrated the sensors' position concerning the robot's coordinate frame that we call *base_link*, following the ROS standard. Figure 3 shows the reference frame of each sensor.

3.2.1. Extrinsic parameters. The Jackal robot platform has the position of the internal sensors factory calibrated, so we need to calibrate only the added sensors, in this case, the LIDAR and both cameras.

We use Kalibr (Furgale et al., 2013) to calibrate the relative transformation between the camera and the IMU. They presented a framework to estimate the temporal offset between the measurement of different sensors and their (relative) spatial transformation.

We use Beltrán et al. (2022) work to calibrate the relative pose between the LIDAR and the camera. To that end, we constructed a calibration board. First, the method uses LIDAR and stereo-extracted referenced points, and then we optimize the transformation of both point sets.

3.2.2. Intrinsic parameters. To calibrate Jackal's internal IMU, we used the *calibrate_compas* node from Clearpath. The robot started to rotate slowly in place for 60 s, recording

magnetometer data, then computed magnetic calibration and generated a (YAML) configuration file. Due to the factory's recommendation,[2] we do not calibrate ZED2 cameras. The manufacturers did an extensive and rigorous multi-step factory calibration.

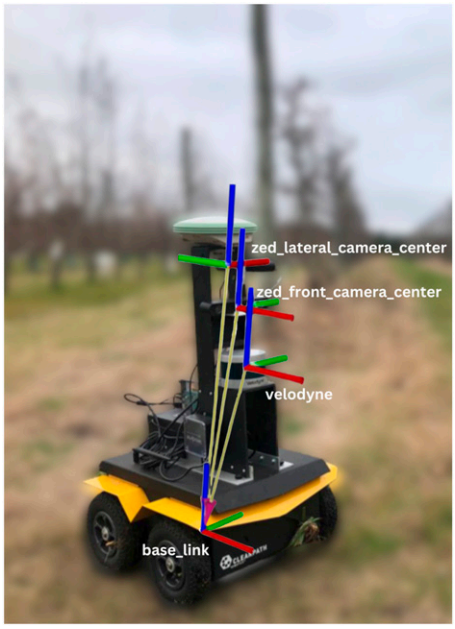

Figure 3. Robot's sensor coordinate frame. Red is the *x*-axis, green the *y*-axis, and blue the *z*-axis.

4. Dataset

In this section, we describe the data acquisition process, the dataset's structure, the method to download, and the instructions to use it.

4.1. Data acquisition

We started collecting data in June 2022 at an experimental station of the National Institute of Agricultural Research (INIA), Las Brujas, Canelones, Uruguay. Specifically, we collect data on an apple and pear field under different climatic conditions and over different plant growth stages (see Figure 4). All the trajectories are made in two field sectors to have variety in the type of crops, as shown in Figure 5.

The robot is driven in hybrid (manual and autonomous) mode; it navigates autonomously between the rows of trees, staying in the center of the rows using the laser's data. For this, we implemented a ROS node that processes the laser's point cloud and filters it, keeping only the points on the robot's left side. We find the line that best fits those points and compute the appropriate velocity vector to stay parallel to that line at a preset distance. At the end of the row, the robot goes into manual mode; in this mode, a person controls the robot using a joystick to make the turn determined by the experimental protocol.

The robot always follows the same path for data acquisition, even in different sectors. The trajectory is

Figure 4. Example of two images acquired by the robot in the same position with different weather conditions.

Figure 5. First GPS trajectories made during data collection. The first image shows the two different sectors where the data was taken (green and red), and the other two images show a zoom-in on these trajectories.

designed so that the robot transits the same places in one direction and the opposite (see Figure 6). That is especially important to evaluate SLAM algorithms, in particular loop closures. In addition, the path is planned so that the robot moves from both sides of the same row of plants. Table 2 summarizes trajectory information, and Figure 7 illustrates images acquired.

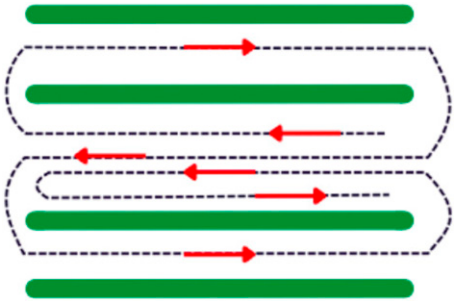

Figure 6. The figure shows the trajectory made by the robot. The thick green lines represent the rows of trees, the black dotted line represents the robot's path, and the red arrows show the robot's direction.

4.2. Data structure

The collected data is saved in ROS bag format. For practicality, the data can be downloaded individually. Each file represents a single trajectory at a specific moment. GPS data is saved in two different formats for convenience use; one on Cartesian WGS84 mode formatted as *timestamp x y z*; and the other as TUM format (Klenk et al., 2021), where each row has a position formatted as timestamp (the number of seconds since the Unix epoch), position concerning to the world origin, and orientation as a quaternion, separated by a space: *timestamp* $x\ y\ z\ q_x\ q_y\ q_z\ q_w$. The GPS has no orientation, so the orientation is always 0 0 0 1. The data (with the exception of the LIDAR, that is, only in ROS format) is also available in raw format as follows:

- **Images:** The images are saved in *JPEG* format inside two folders, one for the front stereo camera and one for the side stereo camera. The left and right images of the corresponding stereo camera are saved inside each folder, denoting in the filename the associated timestamp and which camera captured the images (*left*_[*timestap*]. *JPEG* or *right*_[*timestamp*]. *JPEG*).

Table 2. Description of each trajectory. Sectors S1 and S2 are depicted in red and green in Figure 5, respectively. The sequence name represents, first, the sector (S1 or S2) followed by a dash and the date in *yymmdd* format. (*) This trajectory is only the first loop.

Sequence	Length (m)	Duration (s)	Sector	Description
S1-220706	385	1442	S1	Winter, leafless trees, no fruit, cloudy, morning.
S2-220706	386	1467	S2	Winter, leafless trees, no fruit, cloudy, morning.
S1-220622	370	2042	S1	Winter, almost leafless trees, no fruit, cloudy, morning.
S2-220622 (*)	184	1025	S2	Winter, almost leafless trees, no fruit, cloudy, morning.
S1-221013	393	1452	S1	Spring, medium leafs, flowers, no fruit, cloudy, afternoon.
S2-221013	389	1413	S2	Spring, medium leafs, no fruit, cloudy, afternoon.
S1-221205	364	1333	S1	Spring, leaf trees, small fruit, sunny, noon.
S2-221205	394	1486	S2	Spring, leaf trees, small fruit, sunny, noon.
S1-230228 (*)	199	657	S1	Summer, leaf trees, big fruit, sunny, afternoon.

Figure 7. Sample images of dataset sequences according to the time of year of acquisition. It is possible to see the enormous variation that the trees go through during the course of the year. (a) February. (b) June. (c) July. (d) October. (e) December.

- **IMU**: The file contains the timestamp, angular velocity, and linear acceleration with their covariance. Also, the orientation is in quaternion format.
- **Wheel odometry:** The linear displacement estimations from the encoder-fused odometry are saved as pose (position and orientation) and twist (linear and angular)

5. Experimental evaluation

In order to validate the dataset, we compared two state-of-the-art SLAM algorithms, one using the stereo cameras: RTAB-Map (Labbé and Michaud, 2019), and one using LIDAR: Cartographer (Hess et al., 2016). We use all the algorithms with their default parameters. To evaluate the estimated trajectories, we calculate the absolute trajectory error (ATE) defined by Sturm et al. (2012) using the EVO tool (Grupp, 2017).

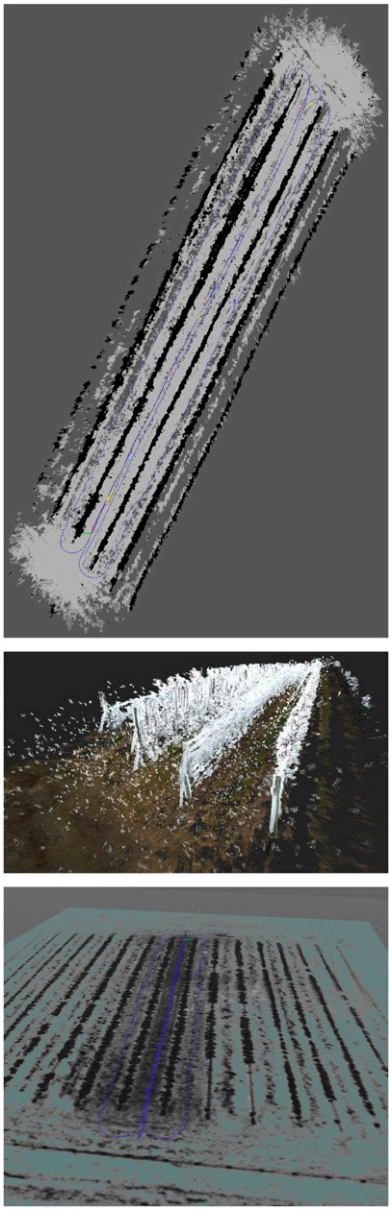

Figure 8. First two images show RTAB-Map's output for the S2220706 trajectory: the generated graph (above), and the reconstructed 3D point cloud (middle). On the bottom, we show Cartographer's map and estimated trajectory for s1220622.

5.1. Test on RTAB-Map

RTAB-Map is a graph-based visual and LIDAR SLAM approach focusing on memory management. The odometry can be an external input, or it could be generated using an RGB-D or stereo camera with the RTAB-Map's visual odometry module. We use the default configuration to validate our visual data (*demo_stereo_outdoor.launch*). As an example, in Figure 8 we show the trajectory graph generated and the reconstructed point cloud. Table 3 shows the absolute trajectory error and Figure 9 shows the reference and estimated trajectory errors for one sequence. It can be seen that S1-230228 presents a greater error, this may be due to the bias presented by the IMU, which we attribute to weather-related high temperatures, and that the robot makes some sudden movements.

5.2. Test on Cartographer

Cartographer is a 2D and 3D SLAM system for multiple platforms and range sensor configurations. To achieve real-time loop closure they use a branch-and-bound approach, generating scan-to-sub-maps matches and constraints. As an example, in Figure 8 we show the trajectory graph generated for one trajectory. Table 3 shows the absolute trajectory error, and Figure 10 shows reference and calculated trajectory error for one sequence. Cartographer relied more heavily on IMU data to use as a prior for scan matching. Bags S1-221205, S1-230228, and S2-221205 present a more pronounced IMU bias, which we attributed to the environment temperature

Table 3. Absolute trajectory error for RTAB-Map and Cartographer on the Magro dataset V-1.0. Missing data for Cartographer is due to the algorithm not converging on a reasonable solution.

Trajectory ID	RTAB-Map Mean ± STD (m)	Cartographer Mean ± STD (m)
S1-220706	0.71 ± 0.54	0.12 ± 0.033
S2-220706	0.33 ± 0.19	0.10 ± 0.036
S1-220622	1.79 ± 0.92	1.07 ± 0.72
S2-220622	1.56 ± 0.97	0.54 ± 0.18
S1-221013	1.25 ± 0.59	1.63 ± 1.38
S2-221013	0.58 ± 0.30	0.12 ± 0.055
S1-221205	1.19 ± 0.93	—
S2-221205	0.92 ± 0.70	—
S1-230228	5.69 ± 2.14	—

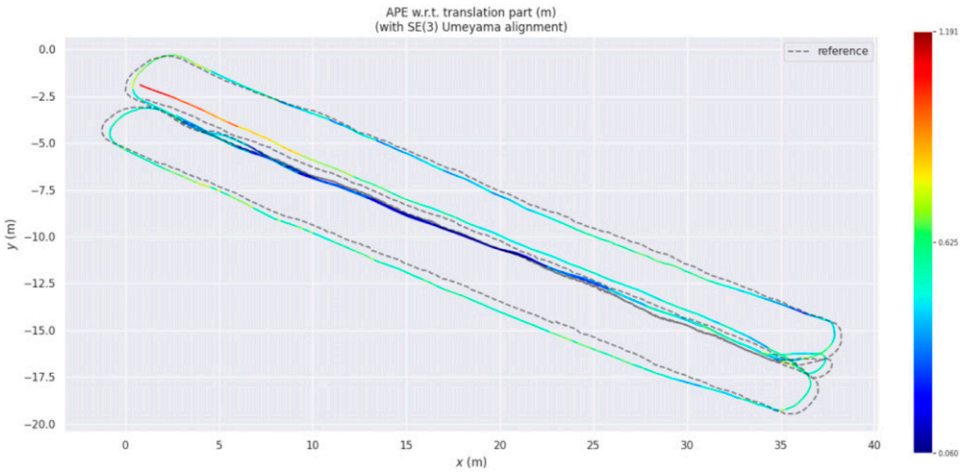

Figure 9. Plots of absolute pose error for trajectories from RTAB-Map using evo_ape tool on S2-220706 trajectory.

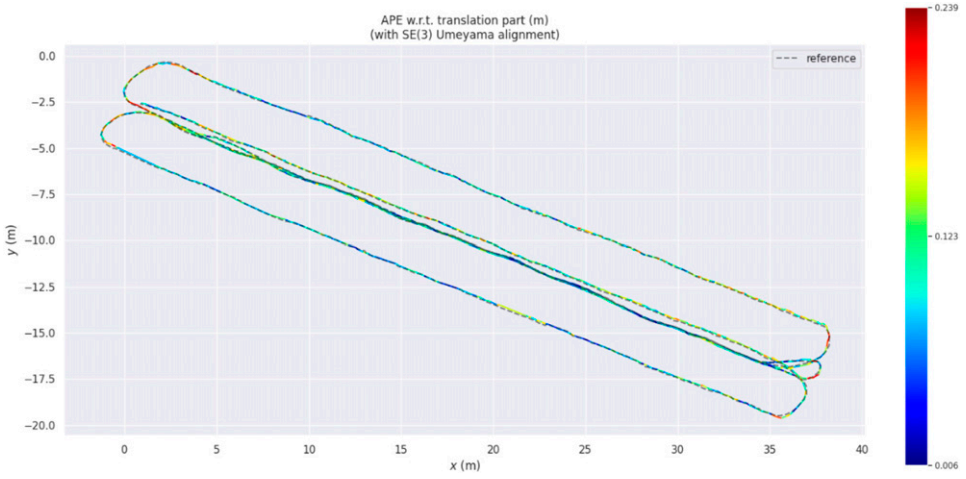

Figure 10. Plots of absolute pose error for trajectories from Cartographer using evo_ape tool on S2-220706 trajectory.

when the data was acquired, around 30°C. Thus, the algorithm does not properly converge in these bags.

6. Conclusions

This paper presents a novel dataset created in challenging natural agricultural settings and aimed at fostering the development of autonomous robots that can boost agricultural industry capabilities. We describe and open-sourced both the collected data and the data collection pipeline. In addition, we test two state-of-the-art SLAM algorithms on the datasets proposed here. Results suggest that the quality of our data is suitable for working with these algorithms. Providing open datasets like the one presented here is of critical importance to enable future research and deployment of autonomous robots in agricultural applications; since these environments present specific, very challenging characteristics (extreme illumination variations, weather, and seasonal changes).

In particular, this dataset allows the community to develop and test SLAM algorithms in agricultural environments, especially between trees. The ability to create a map while accurately locating itself on it is essential for all the tasks that a robot must perform in the field, such as estimating the quantity and quality of fruits, geolocalized detection of pests or weeds, localized application of chemicals, pruning, etc.

The proposed framework is intended to work as a database repository, as we keep collecting data on various crops through the different seasons of the year in the context of a 3-year research project. It is important to note that one of the objectives is to collect data more frequently, seeking to have a continuous data set to work with changing environments with shorter time intervals between data sequences.

One of the following steps will be to explore the possibility of adding a camera to the right or a 360° camera to have a vision on all sides or at least from both sides. We will also try to change the camera for one more that is robust to

sudden lighting changes, aiming at improving the images to, for example, detect the quality of the fruits. In this sense, we will also seek to overcome technical problems to record the data in the highest possible quality, avoiding lossy compression. An additional improvement is to adapt the dataset to ROS2. Although this dataset was created for SLAM tasks, it has the potential to be used for other tasks, so an interesting contribution could be to add semantic information such as fruits, trunks, paths, etc.

The focus of the present work is to propose, share and describe a unique dataset with the potential to help researchers develop novel vision-based techniques and benchmark existing ones. It is outside of the scope of this work to compare and analyze the performance of existing methods, and results depicted in Section 5 are provided as baseline references that researchers can use as sanity checks and benchmarking starting points.

Declaration of conflicting interests

The author(s) declared no potential conflicts of interest with respect to the research, authorship, and/or publication of this article.

Funding

The author(s) disclosed receipt of the following financial support for the research, authorship, and/or publication of this article: This work was partially supported by the project POS_FMV_2021_1_1010856 of the National Research and Innovation Agency of Uruguay (ANII) and the Universidad de la República.

ORCID iDs

Mercedes Marzoa Tanco https://orcid.org/0000-0002-3660-5656
Guillermo Trinidad Barnech https://orcid.org/0009-0009-4328-7877
Javier Baliosian https://orcid.org/0000-0003-1867-5682
Martin LLofriu https://orcid.org/0000-0003-1302-3394

Notes

1. https://gitlab.fing.edu.uy/mmarzoa/magro-dataset
2. https://support.stereolabs.com/hc/en-us/articles/360011828773-How-do-I-recalibrate-my-ZED-stereo-camera-

References

Aghi D, Cerrato S, Mazzia V, et al. (2021) Deep semantic segmentation at the edge for autonomous navigation in vineyard rows. In: 2021 IEEE/RSJ international conference on intelligent robots and systems (IROS), Prague, Czech Republic, 27 September 2021–01 October 2021, pp. 3421–3428. IEEE.

Altaheri H, Alsulaiman M, Muhammad G, et al. (2019) Date fruit dataset for intelligent harvesting. *Data in Brief* 26: 104514.

Barth R, Ijsselmuiden J, Hemming J, et al. (2018) Data synthesis methods for semantic segmentation in agriculture: a capsicum annuum dataset. *Computers and Electronics in Agriculture* 144: 284–296.

Beltrán J, Guindel C, de la Escalera A, et al. (2022) Automatic extrinsic calibration method for lidar and camera sensor setups. *IEEE Transactions on Intelligent Transportation Systems* 23(10): 17677–17689.

Burri M, Nikolic J, Gohl P, et al. (2016) The EuRoc micro aerial vehicle datasets. *The International Journal of Robotics Research* 35(10): 1157–1163.

Chebrolu N, Lottes P, Schaefer A, et al. (2017) Agricultural robot dataset for plant classification, localization and mapping on sugar beet fields. *The International Journal of Robotics Research* 36(10): 1045–1052.

Choi T, Guevara D, Bandodkar G, et al. (2023) Davis-ag: a synthetic plant dataset for developing domain-inspired active vision in agricultural robots. arXiv preprint arXiv: 2303.05764.

Cortés S, Solin A, Rahtu E, et al. (2018) Advio: an authentic dataset for visual-inertial odometry. In: Proceedings of the European conference on computer vision (ECCV), Munich, Germany, 8–14 September 2018, pp. 419–434.

Curnis G, Fontana S and Sorrenti DG (2022) Gtasynth: 3d synthetic data of outdoor non-urban environments. *Data in Brief*: 43: 108412.

de Silva R, Cielniak G and Gao J (2021) Towards agricultural autonomy: crop row detection under varying field conditions using deep learning. arXiv preprint arXiv: 2109.08247.

Dhanasekar J, Sathish Kumar B, Akash S, et al. (2022) Design and implementation of a weed removal agriculture robot. In: International conference on electrical and electronics engineering, London, UK, 6–8 July 2022, pp. 541–550. Springer.

Di Cicco M, Potena C, Grisetti G, et al. (2017) Automatic model based dataset generation for fast and accurate crop and weeds detection. In: 2017 IEEE/RSJ international conference on intelligent robots and systems (IROS), Vancouver, BC, 24–28 September 2017, pp. 5188–5195. IEEE.

Furgale P, Rehder J and Siegwart R (2013) Unified temporal and spatial calibration for multi-sensor systems. In: 2013 IEEE/RSJ international conference on intelligent robots and systems, Tokyo, Japan, 03–07 November 2013, pp. 1280–1286. IEEE.

Geiger A, Lenz P, Stiller C, et al. (2013) Vision meets robotics: the kitti dataset. *The International Journal of Robotics Research* 32(11): 1231–1237.

Gongal A, Karkee M and Amatya S (2018) Apple fruit size estimation using a 3d machine vision system. *Information Processing in Agriculture* 5(4): 498–503.

Griffith S, Chahine G and Pradalier C (2017) Symphony lake dataset. *The International Journal of Robotics Research* 36(11): 1151–1158.

Grupp M (2017) Evo: python package for the evaluation of odometry and slam. https://github.com/MichaelGrupp/evo.

Häni N, Roy P and Isler V (2020) Minneapple: a benchmark dataset for apple detection and segmentation. *IEEE Robotics and Automation Letters* 5(2): 852–858.

Hess W, Kohler D, Rapp H, et al. (2016) Real-time loop closure in 2D LIDAR SLAM. In: 2016 IEEE international conference on robotics and automation (ICRA), Stockholm, Sweden, 16–21 May 2016, pp. 1271–1278. IEEE.

Hroob I, Polvara R, Molina S, et al. (2021) Benchmark of visual

and 3d lidar slam systems in simulation environment for vineyards. In: Towards autonomous robotic systems: 22nd annual conference, TAROS 2021, Lincoln, UK, 8–10 September 2021, pp. 168–177. Springer.

Kierdorf J, Junker-Frohn LV, Delaney M, et al. (2023) Growliflower: an image time-series dataset for growth analysis of cauliflower. *Journal of Field Robotics* 40(2): 173–192.

Klenk S, Chui J, Demmel N, et al. (2021) Tum-vie: the tum stereo visual-inertial event dataset. In: International conference on intelligent robots and systems (IROS), Prague, Czech Republic, 27 September 2021–01 October 2021. IEEE.

Labbé M and Michaud F (2019) Rtab-map as an open-source lidar and visual simultaneous localization and mapping library for large-scale and long-term online operation. *Journal of Field Robotics* 36(2): 416–446.

Lopez-Castro A, Marroquin-Jacobo A, Soto-Amador A, et al. (2020) Design of a vineyard terrestrial robot for multiple applications as part of the innovation of process and product: preliminary results. In: 2020 IEEE international conference on engineering Veracruz (ICEV), Boca del Rio, Mexico, 26–29 October 2020, pp. 1–4. IEEE.

Lu Y and Young S. (2020) A survey of public datasets for computer vision tasks in precision agriculture. *Computers and Electronics in Agriculture* 178: 105760.

Maddern W, Pascoe G, Linegar C, et al. (2017) 1 year, 1000 km: the oxford robotcar dataset. *The International Journal of Robotics Research* 36(1): 3–15.

Majdik AL, Till C and Scaramuzza D (2017) The zurich urban micro aerial vehicle dataset. *The International Journal of Robotics Research* 36(3): 269–273.

Miller M, Chung SJ and Hutchinson S (2018) The visual–inertial canoe dataset. *The International Journal of Robotics Research* 37(1): 13–20.

Mogili UR and Deepak B (2018) Review on application of drone systems in precision agriculture. *Procedia Computer Science* 133: 502–509.

Pawlowski A, Sánchez-Molina J, Guzmán J, et al. (2017) Evaluation of event-based irrigation system control scheme for tomato crops in greenhouses. *Agricultural Water Management* 183: 16–25.

Perez-Borrero I, Marin-Santos D, Gegundez-Arias ME, et al. (2020) A fast and accurate deep learning method for strawberry instance segmentation. *Computers and Electronics in Agriculture* 178: 105736.

Pire T, Mujica M, Civera J, et al. (2019) The rosario dataset: multisensor data for localization and mapping in agricultural environments. *The International Journal of Robotics Research* 38(6): 633–641.

Polvara R, Mellado SM, Hroob I, et al. (2022) Collection and evaluation of a long-term 4d agri-robotic dataset. arXiv preprint arXiv: 2211.14013.

Pronobis A and Caputo B (2009) Cold: the cosy localization database. *The International Journal of Robotics Research* 28(5): 588–594.

Roldán JJ, del Cerro J, Garzón-Ramos D, et al. (2018) Robots in agriculture: state of art and practical experiences. *InTech*. doi: 10.5772/intechopen.6987

Ros G, Sellart L, Materzynska J, et al. (2016) The synthia dataset: a large collection of synthetic images for semantic segmentation of urban scenes. In: Proceedings of the IEEE conference on computer vision and pattern recognition, Las Vegas, NV, 27–30 June 2016, pp. 3234–3243.

Smitt C, Halstead M, Zaenker T, et al. (2021) Pathobot: a robot for glasshouse crop phenotyping and intervention. In: 2021 IEEE international conference on robotics and automation (ICRA), Xi'an, China, 30 May 2021–05 June 2021, pp. 2324–2330. IEEE.

Sturm J, Engelhard N, Endres F, et al. (2012) A benchmark for the evaluation of rgb-d slam systems. In: 2012 IEEE/RSJ international conference on intelligent robots and systems, Vilamoura-Algarve, Portugal, 7–12 October 2012, pp. 573–580. IEEE.

Wang S, Yue J, Dong Y, et al. (2020a) A synthetic dataset for visual slam evaluation. *Robotics and Autonomous Systems* 124: 103336.

Wang W, Zhu D, Wang X, et al. (2020b) Tartanair: a dataset to push the limits of visual slam. In: 2020 IEEE/RSJ international conference on intelligent robots and systems (IROS), Las Vegas, NV, 24 October 2020, pp. 4909–4916. IEEE.

Wang R, Liu L, Xie C, et al. (2021) Agripest: a large-scale domain-specific benchmark dataset for practical agricultural pest detection in the wild. *Sensors* 21(5): 1601.